ELSEVIER

Polymer 41 (2000) 2419–2430

polymer

Thermotropic copolyesters containing spirobicromane moieties: synthesis and primary characterizations

L.-L. Lin, J.-L. Hong*

Department of Materials Science and Engineering, National Sun Yat-Sen University, Kao-hsiung 80424, Taiwan, ROC

Received 22 January 1999; received in revised form 27 April 1999; accepted 7 June 1999

Abstract

Spirobicromane (SPI) are supposed to have a drastic influence on the mesomorphism due to their rigid, bent geometry and bulkiness; therefore, we attempted to build the SPI unit into conventional thermotropic polyester and examine its effect on mesomorphism. In this study, thermotropic copolyester series I and II, with their SPI moieties aggregated or evenly distributed in the polymer chain, can be prepared according to single- and two-step polycondensation reactions of different amounts of SPI, 1,7-heptanediol (HD), and terephthaloyl bis(4-oxybenzoyl chloride) (TOBC), respectively. Thermal transition temperatures (T_m and T_i) for both copolyester I and II series decreased with the increasing SPI moieties incorporated and no liquid crystalline properties were observed for copolyesters with SPI content more than 20 mol%. With more aggregated SPI moieties in the chain, copolyester I series possess higher isotropization temperature and better smectic order as compared to copolyesters II of the same composition, in which the detrimental SPI moieties are assumed to be evenly distributed to efficiently prevent an ordered chain packing in the mesomorphic state. © 1999 Elsevier Science Ltd. All rights reserved.

Keywords: Thermotropic copolyesters; Spirobicromane; Comonomer sequence distribution

1. Introduction

There has been much research on the synthesis of thermotropic polyesters [1–3] and a wide variety of systems, each with unique thermal and physical properties, already exist and are finding applications. Among them, the wholly aromatic thermotropic polyesters generally have high crystal-to-mesophase transitions, T_m, [4,5] and are insoluble in most organic solvents. To obtain polymers with considerably low T_ms, several chemical modifications including: (i) the introduction of bulky, or non-symmetrical substituents; (ii) the use of flexible spacer; (iii) the use of non-linear or bent monomers; and (iv) copolymerization of different monomers [6–13] had been previously used. Route of copolymerization provides versatile ways to prepare new thermotropic copolyesters through the use of conventional monomeric diacids and diols.

Several research studies on the syntheses of thermotropic copolyesters had been previously described [14–19]. Among them, the alternating, block, and random copolymers containing the rigid terephthaloyl bis(4-oxybenzoyl) (TOBC) and butylene terephthalate (BT) flexible units were prepared and systematically studied by Ignatious et al. [18,19]. The resulting block copolyesters exhibit microphase-separated liquid crystalline domain morphology, even at low content of mesogenic unit. In cases of alternating and random copolyesters, the formation and the stability of the mesophase depend on the content of the flexible units, that is, the liquid crystalline properties are lost if the BT content is above 65%. Therefore, the sequence of the constituent units in the polymer chain has a strong effect on the mesomorphism exhibited in the thermotropic copolyesters.

In this study, polycondensation reactions of spirobicromane (SPI, Fig. 1), 1,7-heptanediol (HD), and TOBC (Fig. 1) were performed to prepare copolyesters and their properties were primarily surveyed. Here, use of spiro SPI monomer is due to its rigid, bent geometry imposed by the central quaternary carbon and its steric bulkiness (cf. the simulated structure in Fig. 1). Aligned chain packing around the SPI-rich segments would be conceivably difficult in considering the bent structure of SPI units. Previously, several spiral aromatic diols had been used to construct polyamides, polyimides, and polyesters [20–24]. Among them, aromatic polyesters and copolyesters [24] prepared from combined monomers of 3-(4-hydroxyphenyl)-1,1,3-trimethyl-5-indanol, bisphenol A, isophthaloyl and terephthaloyl chloride were amorphous materials and readily soluble in common organic solvents. This example clearly illustrated

---

* Corresponding author. Tel.: + 886-7525-4065; fax: + 886-7525-4099.
E-mail address: jlhong@mail.nsysu.edu.tw (J.-L. Hong)

PII: S0032-3861(99)00408-5

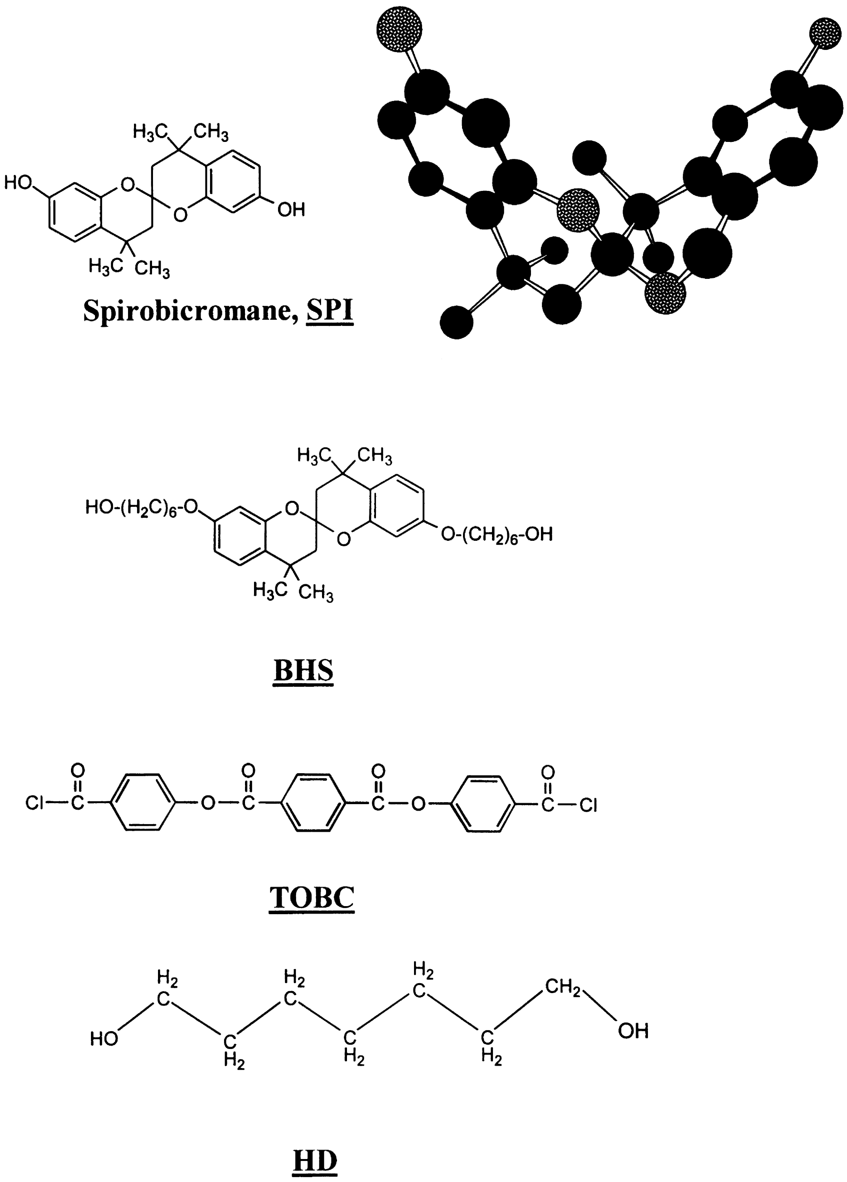

Fig. 1. Chemical structures of SPI (with the ball-and-stick model simulated from ChemDraw 3D), 1,7-heptanediol (HD), and terephthaloyl bis(4-oxybenzoyl chloride) (TOBC).

the effect of the spiro compounds in decreasing the packing tendency of polymer chain; hence, we attempted to prepare thermotropic polyester with the built-in SPI unit and study its influence on the chain orientation in the mesomorphic state. Here, we have chosen polyester system prepared from HD and TOBC monomers in view of the reported low thermal transitions ($T_m = 176°C$, $T_i = 253°C$) and wide mesomorphic range ($\Delta T = 77°C$) [25], properties required for clearer characterizations on the mesomorphism once SPI was incorporated. By a single- and two-stage addition process of the monomeric diols, as shown in Schemes 1 and 2, respectively, copolyesters with its SPI moieties distributed along the polymer main chain in either a more blocky or disperse way can be prepared and characterized. In both polymer I and II series, different amounts of SPI were used to qualitatively estimate its effect on the liquid crystalline properties. All the copolyesters mentioned above have different constituent sequence in the polymer chain, and were characterized by infrared spectroscopy (IR), differential scanning calorimetry (DSC), optical polarizing microscopy (POM), and wide-angle X-ray diffraction (WAXD) in the following discussion.

2. Experimental

2.1. Materials and instrumentation

Terephthaloyl chloride and *p*-hydroxybenzoic acid were recrystallized from hexane and distilled water, respectively.

Pyridine was distilled after dehydration with KOH. 1,7-Heptanediol was vacuum dried at 50°C for 12 h and stored over molecular sieve 4 Å (Linde). 1,1,2,2-Tetrachloroethene (TCE) was pre-dried over molecular sieve 4 Å (Linde) for at least one week before use. Spirobicromane (SPI, Tokyo Chem. Inc., > 99%) and thionyl chloride (Ferak, 99%) were used directly without purification.

The inherent viscosity of all polymers were measured at a concentration of 0.5 g/dl in TCE, using a Ubbelohde viscometer at 30°C. ^{1}H NMR was recorded with a VXR-300 FT-NMR 300 MHz model. Tetramethylsilane (TMS) was used as the internal standard in all cases. A Biorad FTS-40 Fourier-transform infrared spectrometer was used. Spectra in the optical ranges of 4000–400 cm^{-1} were obtained by averaging 64 scans at a resolution of 2 cm^{-1}. All solid samples were mixed with KBr to make pellets for infrared measurement. The texture of the liquid crystals was observed with a Nikon Optiphot-POL microscope equipped with a Linkam TMS controller and THMS 600 hot stage. Phase transition temperatures were detected with a Perkin–Elmer DSC 7 model (scanning rate = 20°C/min). The carrier gas was nitrogen at a flow rate of ca. 10 ml/min. Calibration of the calorimeter was conducted for each heating rate using an indium standard. Temperature-programming X-ray diffraction was performed with a Siemens Diffraktometer D 5000 model with Ni-filtered K_α radiation. The system was evacuated to a pressure of 10^{-5} Torr before heating to high temperature.

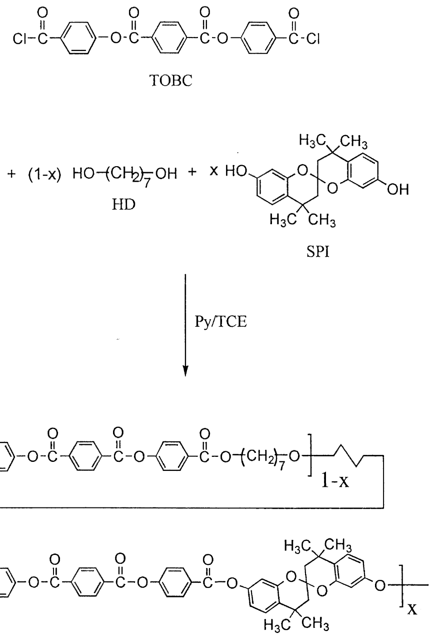

I series **I-19**; x : (1-x) = 1 : 9 **I-46**; x : (1-x) = 4 : 6
I-28; x : (1-x) = 2 : 8 **I-64**; x : (1-x) = 6 : 4

Scheme 1. Syntheses of copolyester I series by a single-step process.

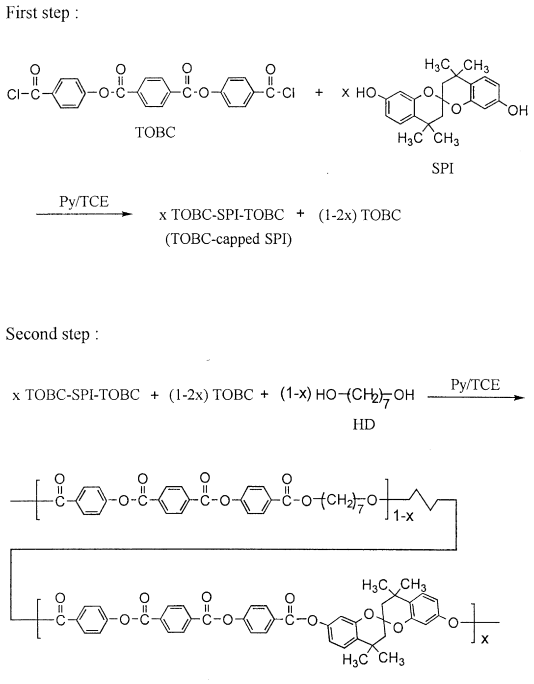

II series **II-06**; x : (1-x) = 0.6 : 9.4
II-19; x : (1-x) = 1 : 9
II-28; x : (1-x) = 2 : 8

Scheme 2. Syntheses of copolyester II series by a two-step process.

2.2. Synthesis

Synthesis of TOBC had been described previously [25,26]. The general synthesis procedures of copolyester I, II series and homopolymers, ST and HT, are given in Schemes 1–3, respectively. All the details are given as in the following sections.

2.2.1. Syntheses of copolyesters I and II series

Syntheses of copolyesters I-19 and II-19 were taken as examples. For syntheses of copolyester II-19, SPI diol (0.9 mmol) in 5 ml of TCE were slowly added dropwise to a solution of TOBC (9 mmol) and catalytic pyridine in 15 ml of TCE under nitrogen atmosphere. The reaction mixtures were then heated at 50°C for 6 h and HD diol (8.1 mmol) in 5 ml of TCE was added to react for another 24 h. In case of copolyester I-19, mixtures of SPI and HD monomers were added to TOBC solution at the same time. The crude product after reaction was precipitated from ethanol, and washed with 5% aqueous HCl, 5% aqueous NaHCO$_3$, 5% aqueous HCl solution, and distilled water. Final polymers were obtained after filtration and dried under vacuum condition. Representative ^{1}H NMR of copolyester I-28 is given later. ^{1}H NMR (300 MHz, CDCl$_3$): δ 8.34 (d, 8 H, terephthalate of triad), 8.26 (d, 4 H, 2,6-*p*-oxybenzoyl of triad connected to SPI moiety), 8.15 (d, 4 H, 2,6-*p*-oxybenzoyl of triad connected to HD moiety),

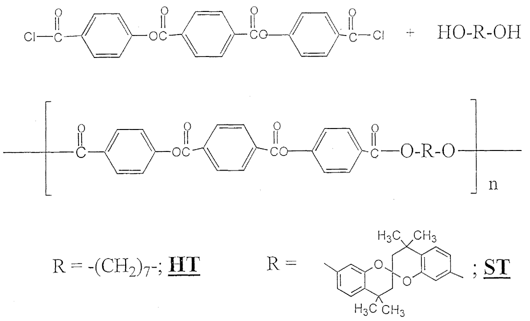

Scheme 3. Syntheses of homopolymers, HT and ST.

7.35 (m, 10 H, 3,5-*p*-oxybenzoyl of triad and 5-*m*-dioxybenzene of the SPI moiety), 6.84 (d, 2H, 4-*m*-dioxybenzene of the SPI moiety), 6.62 (d, 2H, 2-*m*-dioxybenzene of the SPI moiety), 4.36 (t, 4H, $-OCH_2-$), 2.11 (dd, 4H, $-CH_2-$ in the SPI moiety), 1.80 (m, 4 H, $-O-CH_2-CH_2-CH_2-$), 1.62 and 1.40 (s, 12H, $-CH_3$), 1.49 (m, $-O-CH_2-CH_2-(CH_2)_3-CH_2-CH_2-O-$).

2.2.2. Syntheses of homopolyesters, ST and HT

Syntheses of homopolymers, ST and HT, followed the same procedures. Under nitrogen atmosphere, solution of diol monomer (9 mmol of SPI (or HD) in 5 ml of TCE was added dropwise to a solution of TOBC (9 mmol), pyridine (catalytic amounts) in 15 ml of TCE. Reaction was continued at 60°C for 24 h. The crude product was precipitated from ethanol, and washed with 5% aqueous HCl, 5% aqueous $NaHCO_3$, 5% aqueous HCl solution, and distilled water. Final polymers were obtained after filtration and dried under vacuum condition. ^{1}H NMR of HT (300 MHz, $CDCl_3 + CF_3CO_2H$): δ 8.37 (s, 4 H, terephthalate of triad), 8.17 (d, 4H, 2,6-*p*-oxybenzoyl of triad), 7.37 (d, 4H, 3,5-*p*-oxybenzoyl of triad), 4.41 (t, 4H, $-O-CH_2-$), 1.85 (m, 4H, $-O-CH_2-CH_2CH_2-$), 1.49 (m, 6H, $-O-CH_2-CH_2-(CH_2)_3-CH_2-CH_2-O-$). ^{1}H NMR of ST (300 MHz, $CDCl_3 + CF_3CO_2H$): δ 8.40 (s, 4H, terephthalate of triad), 8.29 (d, 4H, 2,6-*p*-oxybenzoyl of triad), 7.41 (m, 6H, 3,5-*p*-oxybenzoyl of triad and 5-*m*-dioxybenzene of the SPI moiety), 6.83 (dd, 2H, 4-*m*-dioxybenzene of the SPI moiety), 6.57 (d, 2H, 2-*m*-dioxybenzene of the SPI moiety), 2.12 (q, 4H, $-CH_2-$), 1.62 and 1.40 (s, 12H, $-CH_3$). IR spectrum (KBr, cm^{-1}): 1742, 1718 ($-C{=}O$ stretching).

3. Results and discussion

Copolyester I and II series were synthesized according to the procedures described in Schemes 1 and 2. Incorporation of the terephthaloyl bis(4-oxybenzoate) (triad, T) moiety in the copolymer was accomplished by polycondensation reactions of TOBC with different amounts of SPI and HD. In this manner, copolyester I and II series were prepared by the single- and two-step pathways described in Schemes 1 and 2, respectively. The two pathways were designed based on the reactivity difference of SPI and HD towards TOBC. Previously, Ignatious et al. [19] had suggested that phenolic hydroxyl groups have higher reactivity than alcoholic hydroxyls towards terephthaloyl chloride; therefore, in the single-step pathway (Scheme 1), SPI would react preferentially and be incorporated into the oligomeric chains formed early in the reaction in higher proportion than its initial mole fraction in the comonomer mixture. The less reactive HD monomer participated in the copolymerization to an increasing extent as the concentration of the more reactive monomer is depleted by the preferential reaction. Thus the copolymer molecules formed contain significant sequences of the same repeat units, i.e. they have a ‘block’ structure. In contrast, copolyesters II from the two-step pathway shown in Scheme 2 should have different constituent sequence. Owing to the excess TOBC applied in the initial stage, a TOBC-capped SPI in combination with the unreacted

Table 1
Primary characterizations for all polymers

Polymer	Mole% of SPI units		Solubility[c]			Inherent viscosity
	Calculated[a]	Found[b]	$CHCl_3$	CH_2Cl_2	TCE	(dl/g)[d]
HT	0	0	−	−	−	–[e]
I-19	0.1	0.11	+	+	+	0.31
I-28	0.2	0.16	+	+	+	0.31
I-46	0.4	0.26	+	+	+	0.23
I-64	0.6	0.58	±	±	±	–[e]
ST	1.0	1.0	−	−	−	–[e]
II-06	0.06	0.04	+	+	+	0.29
II-19	0.1	0.1	+	+	+	0.28
II-28	0.2	0.15	+	+	+	0.27

[a] Mole% of SPI feed in the synthesis step.

[b] Calculated from ^{1}H NMR by measuring the relative peak intensities between aromatic and aliphatic areas.

[c] +: soluble, −: insoluble, and ±: partially soluble.

[d] Inherent viscosity was measured at 30°C with a concentration of 0.5 dl/g in TCE.

[e] Data are not available due to the insolubility of the corresponding polymer in TCE.

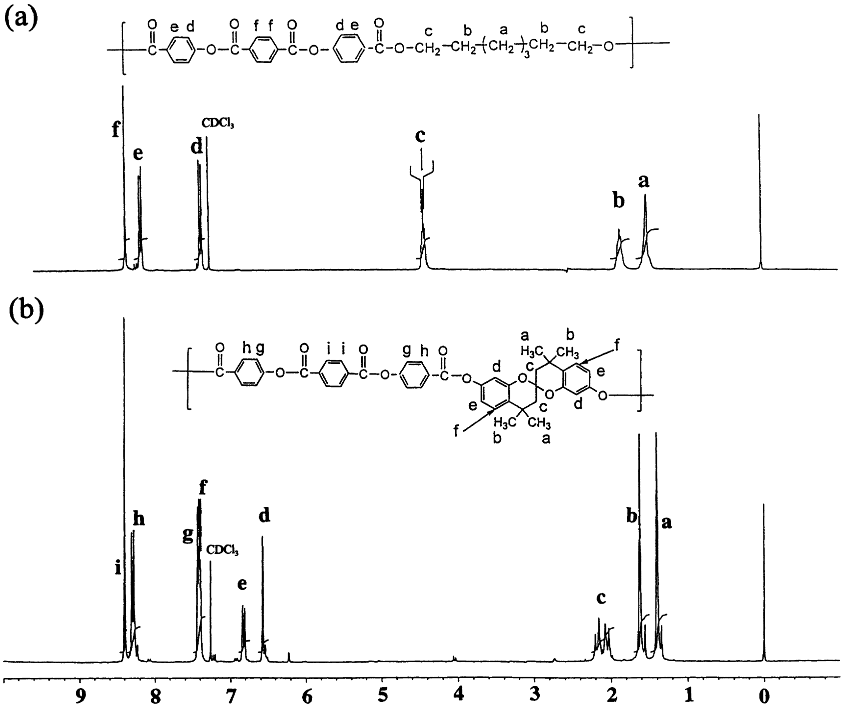

Fig. 2. ^{1}H NMR spectra of homopolymers (a) HT and (b) ST (in $CDCl_3$ + CF_3CO_2H).

TOBC should be generated in the first step and then, the above mixtures further reacted with HD monomer added in the second step to yield copolyester II series, which should have their SPI and HD units distributed more evenly as compared to copolyester I series of the same composition. Due to the variations on the sequence distribution, copolyesters I and II behave differently and will be discussed later. Nomenclatures for copolyesters I and II were based on the molar ratios of the two diols applied in the synthesis step (as indicated in Schemes 1 and 2); for example, one to nine equivalents of SPI to HD diols were used to prepare copolyester I-19. Other homopolymers, ST and HT, synthesized according to Scheme 3 were prepared in order to compare with the copolyesters in the I and II series.

Primary characterization data such as intrinsic viscosity and solubility in chlorinated solvents (i.e. methylene chloride, chloroform, and TCE) are summarized in Table 1. Homopolymers HT and ST are completely insoluble in

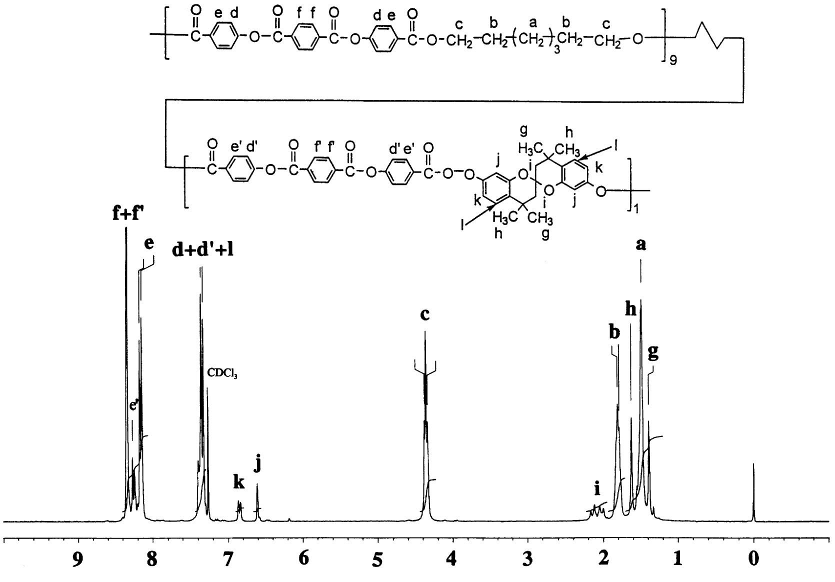

Fig. 3. ^{1}H NMR spectrum of copolyester I-19 (in $CDCl_3$).

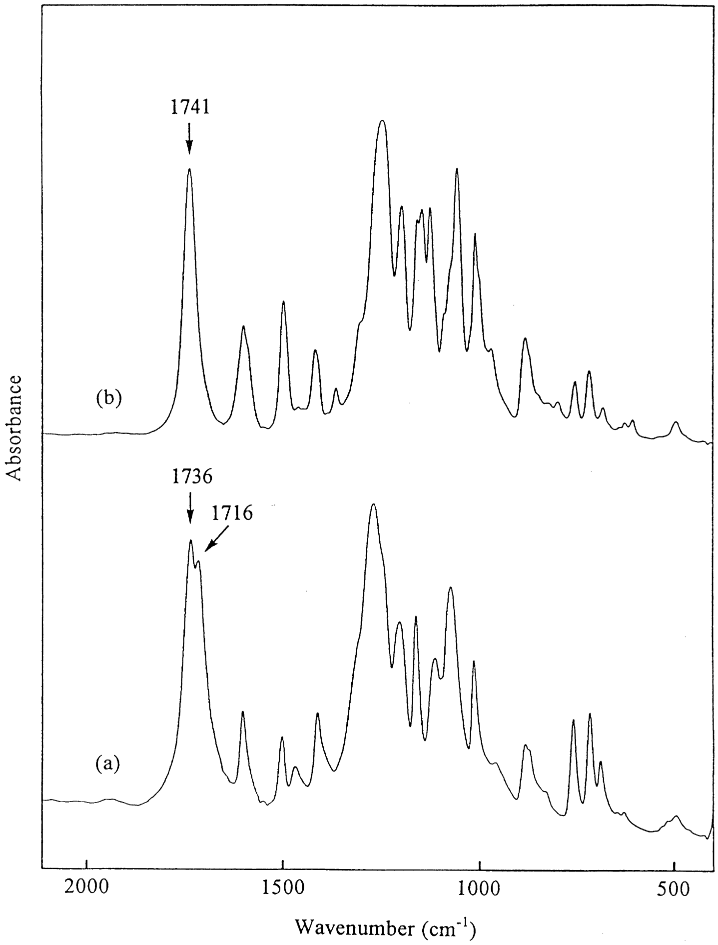

Fig. 4. Infrared spectra of homopolymers (a) HT and (b) ST.

the chlorinated solvents; with the addition of small amounts of SPI comonomer, copolyesters I-19, II-06, and II-19 are all soluble materials. Except copolyester I-64, other copolyesters (i.e. I-28, I-46, and II-28) are readily soluble in the chlorinated solvents, too. The poor solubility for I-64 is probably due to its high content of rigid SPI moieties. The distinguished solubility difference between homopolymers HT, ST and copolyesters I, II is therefore attributed to the comonomer and the destruction effects originated from the rigid SPI units. The constituent sequence difference between copolyester I and II series is expected to cause variations on their mesomorphic properties, and will be discussed following this paper.

^{1}H NMR spectra of homopolymers ST and HT can be used as a basis for the structure identification for copolyester I-19. One drop of CF_3CO_2H was used to help the dissolution of both polymers in $CDCl_3$. The ^{1}H NMR spectrum of homopolymer HT, shown in Fig. 2(a), contained peaks at δ 8.37 (H_f, singlet) and 8.18–8.15 (H_e, doublet) corresponding to the four terephthalate and four 3,5-*p*-oxybenzoyl protons of the triad moiety, respectively; while the corresponding peaks in homopolymer ST (Fig. 2(b)) showed at a lower field of δ 8.40 (H_i, singlet) and 8.31–8.28 (H_h, doublet) due to the deshielding effect from the neighboring phenylene rings of the SPI moieties. The other four 2,6-*p*-oxybenzoyl protons in ST (H_g at δ 7.44–7.42, Fig. 2(b)) also appeared at a lower field than the correlated protons in HT (H_d at δ 7.38–7.36, Fig. 2(a)). Representative example of copolyester I-19 (Fig. 3) therefore possesses all the characteristic peaks from both the –SPI–T– and –HD–T– units in the ranges of δ 8.4–7.3; the rest of the peaks can be also deduced from the spectra of ST and HT homopolymers. Mole percent of the SPI moieties relative to the total diols (SPI and HD) in the resulting copolyesters can be also deduced from the peak intensity ratio between aliphatic and aromatic regions, and the results are listed in Table 1 to compare the feed ratio in the synthesis step. Most of the samples have reasonable correlation between the feed ratio and the calculated value.

Infrared study on HT, ST, and copolyester I-19 was concentrated on the carbonyl (–C=O) stretching modes (Fig. 4). Homopolymer ST exhibits one –C=O absorption band at 1741 cm^{-1}, in contrast to the observed two bands at 1735 and 1713 cm^{-1} for HT homopolymer. Previously, we had conducted infrared study on the liquid crystalline bis[4-(pentyloxycarbonyl)phenylene]terephthalate (BPT) [27],

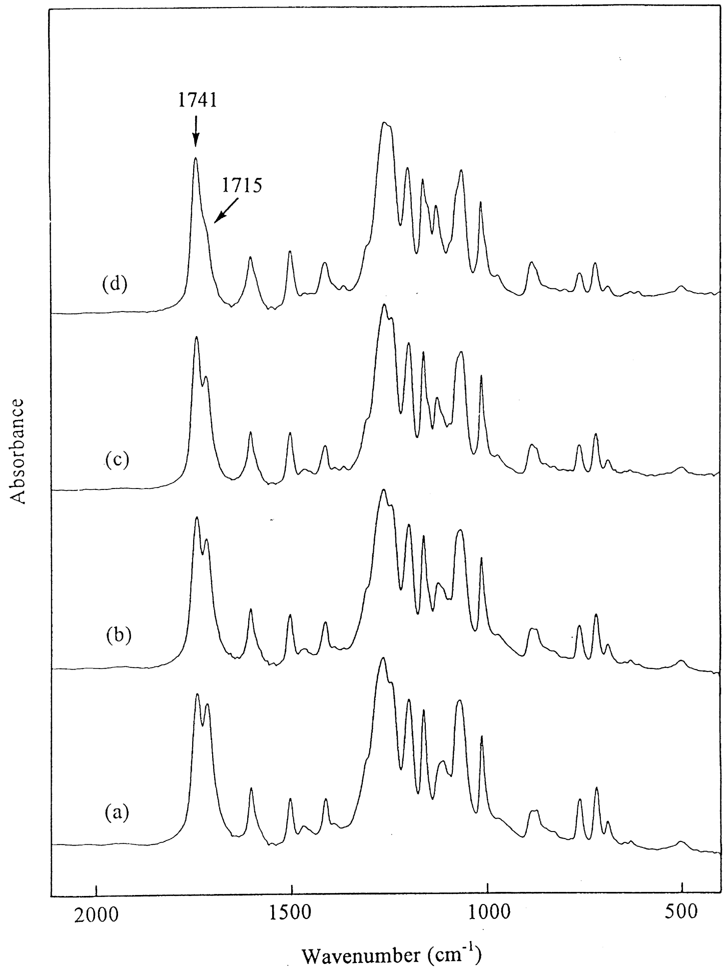

Fig. 5. Infrared spectra of copolyesters: (a) I-19, (b) I-28, (c) I-46 and (d) I-64.

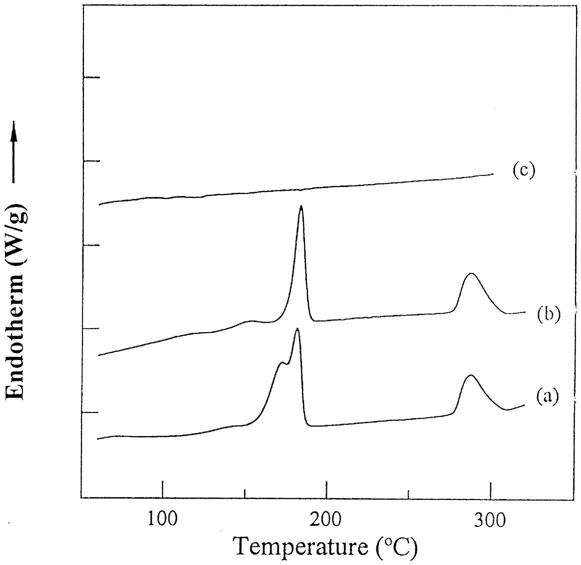

Fig. 6. DSC thermograms of homopolymers: (a) HT (as-reacted); (b) HT after cooling from the isotropic liquid state; and (c) ST (scanning rate = 20°C/min).

and suggested that, in the mesophase, the two –C=O bands at 1743 and 1723 cm^{-1} observed for BPT are attributed to the internal (–Ar–COO–Ar–) and external (–Ar–COO–R) ester –C=O groups, respectively. It means that ester group wedged between two aromatic phenylene rings has its absorption band appearing at higher frequency than ester group neighboring to only one phenylene ring due to the bond length difference of the –C=O bond. This result explains the observed one and two absorption bands for ST and HT polyesters, respectively. Infrared spectra of the selected copolyester I series in Fig. 5(a)–(d) clearly demonstrate the trend that increasing content of SPI resulted in the decreasing external band at ~1715 cm^{-1}. Copolyester II also has two –C=O absorption bands at 1741 and 1715 cm^{-1} with their relative intensity ratios varied by the incorporated SPI amounts.

DSC traces of homopolymers ST and HT, shown in Fig. 6, have different features. As a potentially amorphous material, DSC thermograms of ST homopolymer (Fig. 6(c)) shows no thermal transition below 300°C (continued heating to temperatures above 300°C resulted in decomposition). POM study suggested no mesomorphism

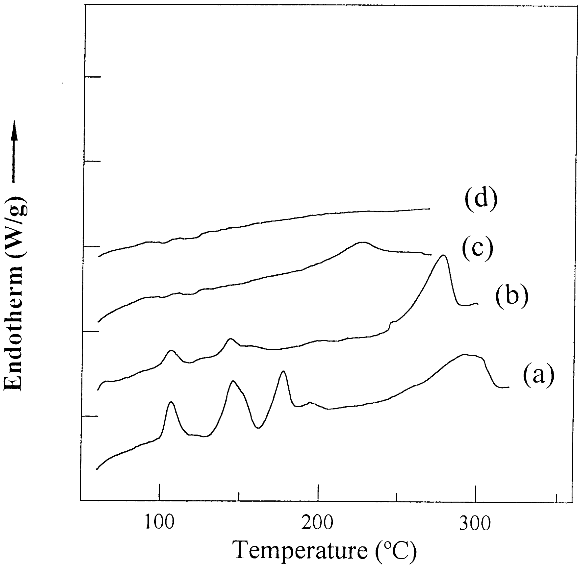

Fig. 7. DSC thermograms of copolyesters: (a) I-19, (b) I-28, (c) I-46 and (d) I-64 (scanning rate = 20°C/min).

at any temperature below decomposition (~320°C). Suggestively, the bulky SPI moieties incorporated in ST effectively retard the crystallization process. In comparison, the as-reacted HT (Fig. 6(a)) exhibited a broad tiny endotherm right before the double melting (T_m ~ 180°C) and the isotropization (T_i ~ 290°C). Second rescan of the HT polymer after quenched from the isotropic liquid state transformed the double melting peaks into one tiny (~150°C) and one major endotherm at a slightly higher position (~176°C) than that obtained in the 1st run, but for T_i transition, it remained intact. Suggestively, different crystal structures induced by the solvent applied in the synthesis step can be eliminated by thermal treatment. Here, peak temperature of T_i is higher than that (T_i = 253°C) reported by Ober et al. [25], however, this difference may be due to different determination methods (by visual observation as they claimed) or molecular weight difference (a lower η_{inh} value of 0.196 was reported in their case). In contrast to the liquid crystalline HT polyester, the rigid ST homopolymer exhibited no mesomorphism under POM inspection, a result possibly due to the detrimental effect of the inherent SPI moieties on chain packing.

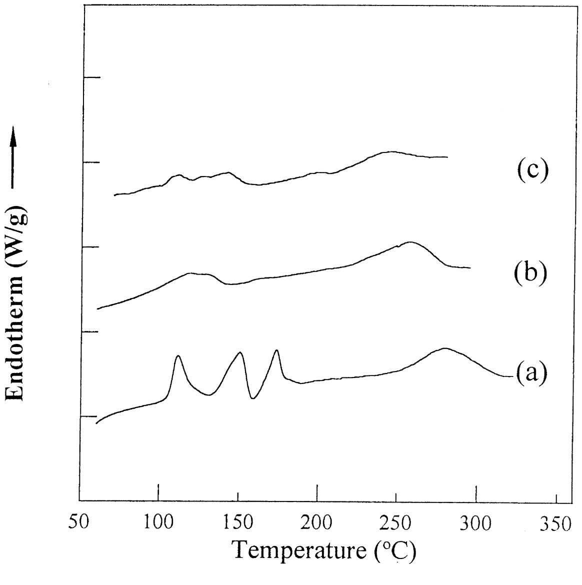

Fig. 8. DSC thermograms of copolyesters: (a) II-06, (b) II-19 and (c) II-28 (scanning rate = 20°C/min).

DSC scans of the copolyester I and II series with varied compositions resulted in different thermograms (Figs. 7 and 8). Copolyester I-19 (Fig. 7(a)), with low SPI content, exhibits multiple melting peaks, and a broad T_i transition with its peak temperature close to HT homopolymer. By appropriate annealing process at 150°C (or 165°C) for 2 h, the multiple melting peaks observed for I-19 became one small, broad peak at ~125°C and one sharp, large peak centered at 182°C; therefore, the multiple-melting behavior for I-19 should not be attributed to the multiple molecular weight distribution generated from the synthesis stage. This statement also holds for copolyesters I-28 and II-06, which also possess multiple-melting behavior. Previously, several publications on the semi-rigid polyester systems had attributed their multiple-melting behavior to different origins, such as reorganization and perfection [28,29], registry of neighboring chain in the mesomorphic state [30,31] or dual crystal [32]. The origins of the multiple-melting behavior for copolyester I-19 had been studied by different isothermal crystallizations and annealing experiments in our laboratory, and will be the topics of our next publication. With a higher SPI content than I-19, copolyester I-28 (Fig. 7(b)) has two small melting peaks, and one T_i transition appeared at lower temperatures than I-19 case. The two melting transitions shown in Fig. 7(b) are approximately at the same temperature ranges but with lower intensities as compared with the two low-temperature melting peaks for copolyester I-19 (Fig. 7(a)). Suggestively, copolyester I-19 possesses certain crystalline domains (corresponding to the meltings of the two high-temperature endotherms in Fig. 7(a)), which are more perfect than the crystalline structures in copolyester I-28. The influence of SPI moieties is even more pronouncing as we inspected thermograms of copolyesters I-46 and I-64, where only a low T_i transition (Fig. 7(c)) or no major transition (Fig. 7(d)) was detected. Further investigation by POM suggested the absence of any mesophase for copolyesters I-46 and I-64. Therefore, SPI-moieties in the copolyesters are detrimental to the chain packing either in the solid or in the liquid crystalline state. DSC thermograms of copolyester II series in Fig. 8 also showed the same trend of decreasing transition temperatures with increasing SPI content. Multiple-melting behavior shown in copolyesters I-19 and I-28 can only be observed in copolyester II-06 (Fig. 8(a)), which has a low SPI content of 4 mol% as determined from ^{1}H NMR. With increasing SPI contents, copolyester II-19 and II-28 have their T_m and

Table 2
Data adapted from DSC scans of copolyester I and II series

Polymer	T_{m3}[a] (°C)	T_{m2}[a] (°C)	T_{m1}[a] (°C)	ΔH_m[b] (J/g)	T_i[c] (°C)	ΔH_i[d] (J/g)	ΔS_i[e] $\times 10^2$ (J/g K)
I-19	109	148	179	16.49	288	14.00	2.51
I-28	109	145	–	3.25	277	12.22	2.22
I-46	–	–	–	–	225	4.59	0.92
I-64	–	–	–	–	–	–	–
II-06	112	150	175	13.57	280	10.98	1.98
II-19	125	–	–	6.45	257	9.70	1.83
II-28	126	–	–	4.84	238	3.71	0.73

[a] T_{mx}: peak temperature of the melting transition, the Arabic numeral x refers to the xth melting transition counting from the higher temperature region.
[b] ΔH_m: total enthalpies of all melting transitions.
[c] T_i: isotropization temperature.
[d] ΔH_i: enthalpy change during isotropization.
[e] ΔS_i: entropy change during isotropization, calculated from $\Delta H_i/T_i$.

T_i transitions appearing at lower temperature ranges and with less involved enthalpies as compared to II-06. Influence of SPI moieties in copolyester II series is basically similar to those in copolyester I series.

Table 2 summarizes the thermal parameters, including peak temperatures, enthalpy (ΔH_i) and calculated entropy (ΔS_i) involved in the isotropization (ΔH_i) steps, adapted from DSC scans. In each series, higher ΔH_i and ΔS_i values are generally observed for copolyesters with less SPI content; also, copolyester in I series has higher values as compared to copolyesters II of the same composition. Primarily, based on the study of Dewar and Griffin [33] on different nematic esters, entropy (ΔS_i) involved during isotropization is determined by both the isotropic temperature (T_i) and entropy changes (ΔH_i), which can be illustrated by $\Delta S_i = \Delta H_i/T_i$. A less-ordered mesophase is probably involved in copolyester II series. Since isotropic liquid state is completely randomized, copolyesters in II series seem to gain more entropy in passing from the mesomorphic to the isotropic liquid state as compared to copolyesters II of the same composition; therefore, a less-ordered mesophase is suggested for copolyester II as compared to copolyester I series.

POM photographs of copolyester I and II series along with HT homopolymer are given in Fig. 9. Homopolymer HT exhibits a broken fan texture (Fig. 9(a)) at 220°C; same texture was also observed for copolyesters I-19 (Fig. 9(b)) but with significantly smaller domain sizes compared to HT. Indistinguishable minute birefringent domains were generated for copolyester I-28 (Fig. 9(c)) with higher SPI content. Comparison can be also made between copolyester I and II series. For the whole copolyester II series, only II-06 (Fig. 9(d)) exhibited clear broken fan texture; for copolyester II-19 (Fig. 9(e)), small mesomorphic texture was observed. With a high SPI content, copolyester II-28 has a texture of scattered birefringent droplets (Fig. 9(f)) over the dark, isotropic background. The presence of dark, isotropic phase, which is still persistent at temperatures conceivably lower than T_i, in polyester II-28 may suggest that the presence of the second phase originated from the amorphous SPI-rich domains and/or the instability of the corresponding mesophase. With a similar composition, copolyester II series seems to have a less-ordered mesophase than I series, a result possibly related to the sequence distribution in each series.

Molecular arrangement of the copolyesters at various temperatures can be evaluated by the temperature-programming WAXD study. Firstly, we examined the diffraction patterns of the homopolymer HT shown in Fig. 10(a). At room temperature, HT possesses three low-angle diffraction peaks at $2\theta = 3.45$, 6.20, and 9.65° and two broad wide-angle peaks at $2\theta = 19.60$ and 23.15°. All the diffraction peaks remained intact at $T = 100$ and 140°C; however, peak in the wide-angle region became broad, and in the low-angle region, two diffraction peaks at $2\theta = 3.6$ (=24.51 Å) and 7.2° (=12.25 Å) were visualized after heating HT to the mesomorphic state (i.e. from 180 to 280°C). The d-spacing of 24.51 Å is close to the reported value of 23.3 Å by Ellis et al. [34]. Previous study on HT [34] (or polyester [35] prepared from diethyl 4,4′-bibenzoate and pentamethylene diol) had proposed a new type of smectic C phase (as smectic C_p or C_2 [36]), in which the mesogenic units in each layer are tilted to the layer normal but with their tilt direction opposite to each other between neighboring layers, to account for the X-ray result. Our result for HT is therefore correlated with the smectic C_2 structure. X-ray diffraction patterns of copolyester I-19 exhibit similar features (Fig. 10(b)) with HT; that is, the two low-angle peaks in the mesophase (in the temperature ranges of 180–240°C) appeared at the same positions of $2\theta = 3.6$ and 7.2°. To compare, diffraction patterns of all copolyesters in their mesophase (at 180°C) are plotted in Fig. 11. In copolyester I series, we observed the significant broadening of peak at $2\theta = 3.6°$ from I-19 to I-28 (cf. Fig. 11(a) and (b)); also, no second order diffraction at $2\theta = 7.2°$ was visible for copolyester I-28. The above observations indicate that a more-ordered smectic C_2 mesophase was generated for copolyester I-19 as compared to I-28; same conclusion can be also drawn as we compare copolyesters II-06 and II-19 (cf. Fig. 11(c) and (d)). Comparison

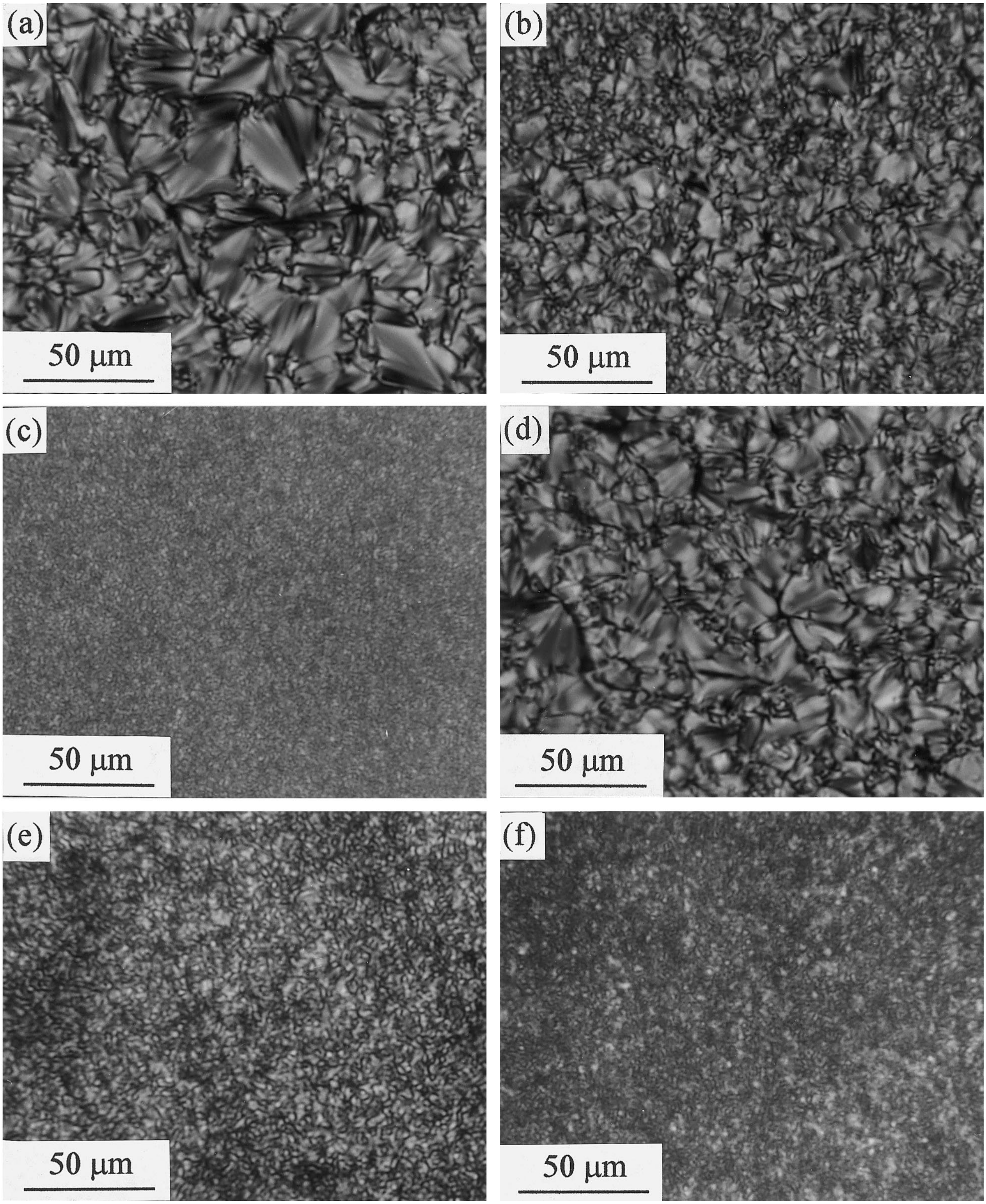

Fig. 9. POM photographs of (a) homopolymer HT; copolyesters: (b) I-19, (c) I-28, (d) II-06, (e) II-19 and (f) II-28 (all photographs were taken at 220°C after cooling from the isotropic liquid state).

can be also made between I and II series, that is, the relative peak broadness suggests that copolyester I-19 possesses a more-ordered smectic mesophase than copolyester II-19, a result indicating the important role of the constituent sequence distribution on the mesomorphism. However, no conclusion can be made between copolyesters I-28 and II-28 since both samples have similar peak broadness (cf. Fig. 11(b) and (e)). The relative mesophase stability

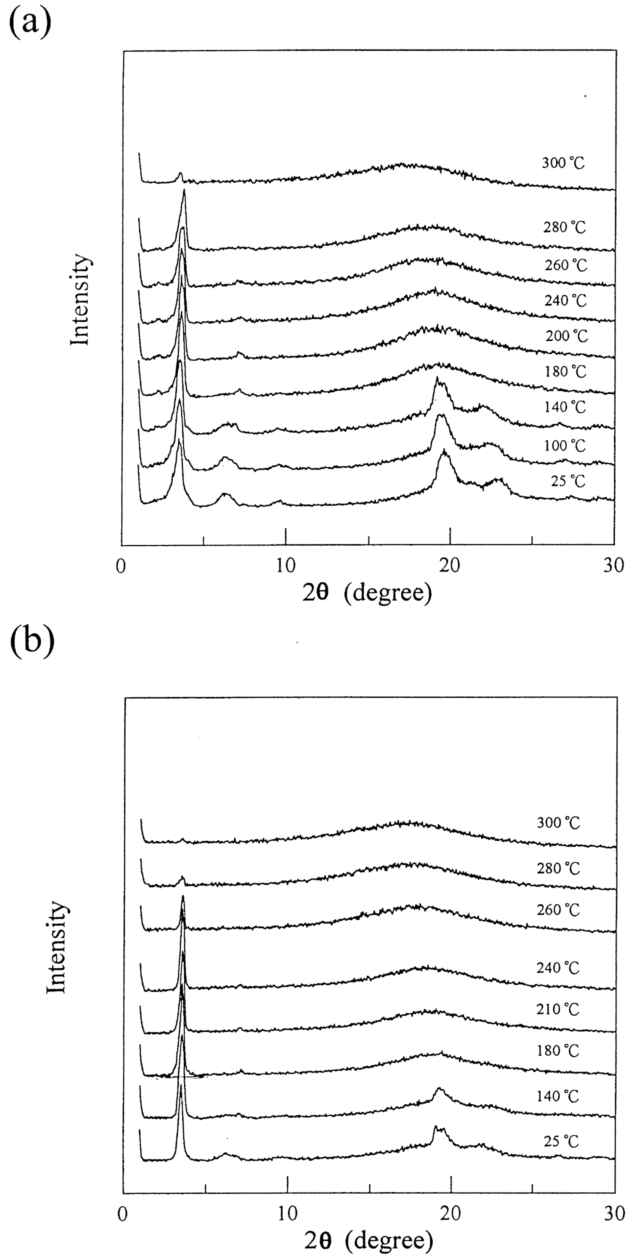

Fig. 10. X-ray diffraction patterns of (a) HT polyester and (b) copolyesters I-19 at various temperatures.

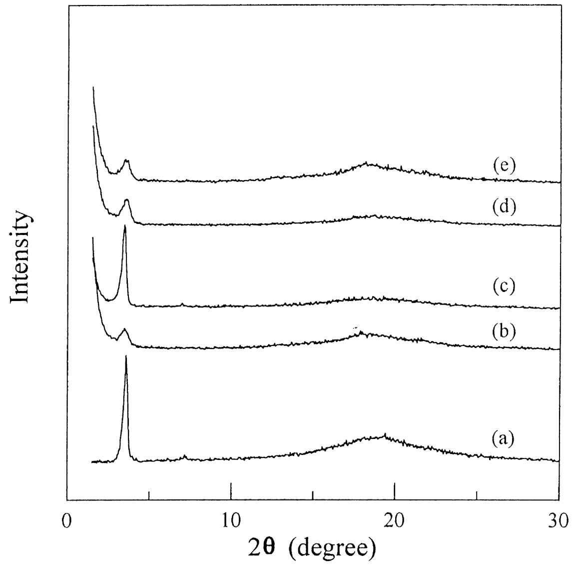

Fig. 11. X-ray diffraction patterns of copolyesters: (a) I-19, (b) I-28, (c) II-06, (d) II-19 and (e) II-28 (all diffractographs were taken at 180°C).

between copolyesters I-28 and II-28 can be concluded from their ΔS_i values (Table 2) as mentioned earlier.

Although the inherent SPI contents in all thermotropic copolyesters is limited, its effect on the mesomorphism is drastic in considering its bulkiness and bent geometry. As suggested from the computer-simulated structure in Fig. 1, SPI moieties would impose a non-linear chain arrangement on the neighboring mesogenic triads, and prevent formation of any ordered, parallel chain arrangement required for smectic layer structure. The effect may be a long range since a bent structure, once formed, may take several neighboring –(TOBC–H)– chain segments to readjust before reaching an ordered smectic layers of considerable dimensions. This argument may provide the reason why copolyesters with more than 20 mol% of SPI (as copolyesters I-46 and I-64) are not liquid crystals. The detrimental effect of SPI moieties for mesomorphism would be more intensive if SPI moieties are more evenly distributed along the polymer chains as in copolyester II series as compared to copolyester I series, where SPI moieties are supposed to be distributed along the chain in a more aggregated manner.

4. Conclusion

By a single- and two-step reaction process, copolyester series I and II with their inherent SPI moieties distributed in a more blocky or even manner can be successfully prepared and their difference on mesomorphism was characterized by DSC, POM, and X-ray diffraction study. In each series, the increasing SPI contents decreases the mesophase stability; with a SPI content more than 20 mol%, copolyesters I-46 and I-64 are not liquid crystals. With the same composition, copolyester II series has a less-ordered mesophase as compared to copolyester I series since II series have their SPI moieties evenly distributed along the corresponding polymer chains.

Acknowledgements

Financial support from the National Science Council, ROC (contract no. NSC 88-2216, E-110-005) is gratefully acknowledged.

References

[1] Jin JI, Ober AC, Lenz RW. Br Polym J 1980;12:132.
[2] Economy J. J Macromol Sci Chem 1984;121:1705.
[3] Varshney SK. Rev Macromol Chem Phys C 1986;26:551.
[4] Strzelecki L, Luyen DV. Eur Polym J 1980;16:299.
[5] Griffin AC, Johnson JE, editors. Liquid crystals and ordered fluids, vol. 4. New York: Plenum Press, 1984.
[6] Krigbaum WR, Hakemi H, Kotek R. Macromolecules 1985;18:965.
[7] Jin JI, Choi EJ, Jo BW. Macromolecules 1987;20:934.
[8] Majnusz J, Catala JM, Lenz RW. Eur Polym J 1983;19:1043.
[9] Ober C, Jin JI, Lenz RW. Polym J 1982;14:9.
[10] Nieri P, Pamiredy C, Wu CN. Macromolecules 1992;25:1796.
[11] Jin JI, Jang JH, Jo BW. Polymer 1992;33:1537.
[12] Navarro F, Serrano JL. J Polym Sci, Polym Chem Ed 1992;30:1789.
[13] Cai R, Samulski ET. Macromolecules 1994;27:135.
[14] Jackson WJ, Kuhfuss HF. J Polym Sci, Polym Chem Ed 1976;14:2043.
[15] Dotrong M, Dotrong MH, Evers RC. Polymer 1993;34:726.
[16] Auman BC, Percec V. Polymer 1988;29:938.
[17] Galli G, Chiellini E, Yagci Y, Serhatli EI, Laus M, Bignozzi MC, Angelon AS. Makromol Chem 1993;14:185.
[18] Ignatious F, Lenz RW, Kantor SW. Macromolecules 1994;27:5248.
[19] Ignatious F, Lu C, Kantor SW, Lenz RW. Macromolecules 1994;27:7785.
[20] Wilson JC. J Polym Sci, Polym Chem Ed 1975;13:749.
[21] Hsiao SH, Yang CY. J Polym Sci, Polym Chem Ed 1997;35:1479.
[22] Hsiao SH, Yang CP, Yang CY. J Polym Sci, Polym Chem Ed 1997;35:1487.
[23] Schmidhauser JC, Longley KL. Polym Prep 1989;30(1):13.
[24] Imai Y, Tassavori S. J Polym Sci, Polym Chem Ed 1984;22:1319.
[25] Bilibin AY, Ten’Kovstev AV, Piraner ON, Skorokhdov SS. Polym Sci USSR 1984;26:2882.
[26] Dimian AF, Jones FN. In: Dickie RA, Labana SS, Bauer RS, editors. Cross-linked polymers, chemistry, properties, and applications, Washington, DC: American Chemical Society, 1988. p. 324.
[27] Lin CH, Hong YL, Yen FS, Hong JL. Liq Cryst 1996;21:609.
[28] Han CD, Chang S, Kim SS. Macromolecules 1994;27:7699.
[29] Marsano E, Salati U, Valenti B. Polymer 1993;34:1232.
[30] Carpaneto L, Marsano E, Valenti B, Zanarde G. Polymer 1992;33:3865.
[31] Carpaneto L, Marsano E, Salati U, Valenti B. Polymer 1993;34:3464.
[32] Cheng Y-Y, Cebe P, Capel M, Scheruder-Gibson H, Bluhm A, Yeomans W. J Polym Sci, Polym Phys Ed 1995;33:2331.
[33] Dewar MJ, Griffin AC. J Am Chem Soc 1975;97:6662.
[34] Ellis G, Lorente J, Marco C, Gomez MA, Fatou JG. Spectrochim Acta A 1991;47:1353.
[35] Helmut RB, Cladis PE, Pleiner H. Macromolecules 1992;25:7233.
[36] Watanabe J, Hayashi M. Macromolecules 1989;22:4083.